SPEEDAM 2008
International Symposium on Power Electronics,
Electrical Drives, Automation and Motion

Losses Calculation for Medium Voltage PWM Current Source Rectifiers using Different Semiconductor Devices

Ahmed K. Abdelsalam , Mahmoud I. Masoud , Stephen J. Finney and Barry W. Williams

Electronic & Electrical Engineering Department, Strathclyde University, Glasgow, UK

***Abstract*-- In this paper, a comparison of losses and size for three semiconductor devices suitable for medium voltage (2.4 kV, 3.3 kV and 6.6 kV) high power applications is presented. The comparison is made for medium voltage PWM current source rectifiers using a selective harmonic elimination technique. The devices compared are High Voltage Insulated Gate Bipolar Transistor (HVIGBT) and two types of hard-driven thyristors, namely, the Symmetrical Gate Commutated Thyristor (SGCT) and the Asymmetrical Gate Commutated Thyristor (AGCT). The study depends on practical devices, data sheets from well known semiconductor vendors, taking into account accurate discrimination between turn-off and recovery states.**

***Index Terms*-- Current source rectifiers, Losses calculations, Medium voltage and Semiconductors.**

INTRODUCTION

Current source rectifiers are frequently used in medium voltage/ high power AC drives. The basic most common types for this front end are either a controlled phase rectifier or a pulse width modulated current source rectifier (PWM-CSR) that is usually modulated with selective harmonic elimination (SHE) techniques as the switching frequency is limited in these applications [1, 2].

The phase-controlled rectifier is simple but requires the connection of a group of passive and/or active filters to accomplish the harmonic and input power factor requirements in a wide operation range [1, 2].

To the contrary, the PWM-CSR harmonic requirements are often accomplished by a simple LC low pass filter, and near unity power factor operation is possible without additional equipment [1]. Fig. 1 shows the basic structure of this type of rectifiers. SHE technique enables the mitigation of low order harmonics with low switching frequency.

The PWM-CSR is modulated using this technique to mitigate the 5th, 7th and 11th harmonics from the input line current. Fig. 2 shows the gating signals for switch S1, (half leg), in a PWM-CSR operating at modulation index (M) equals 1.

In order to achieve the required harmonic elimination stated, each switch in the rectifier is gated by eleven pulses per cycle.

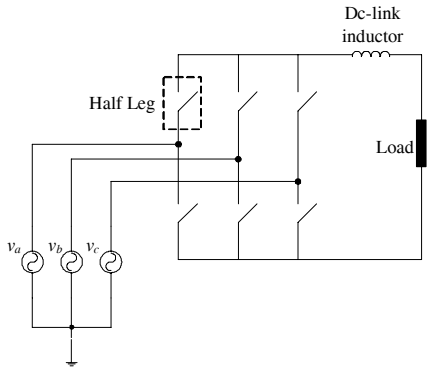

Fig. 1: Basic structure of PWM-CSR

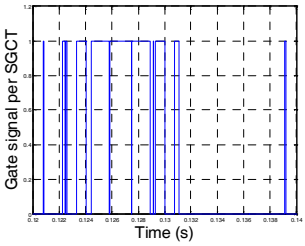

Fig. 2: Gating signal for each half leg of PWM-CSR using SHE technique to mitigate 5th, 7th and 11th of the line current

In this topology of rectifiers, gate turn-off thyristors (GTO) have been used for many years until the middle of 1990. The performance of GTO's was limited by the low switching frequency and the massive snubber components [3]. The evolution of GCT, with its two types symmetrical (SGCT) and asymmetrical (AGCT), opens the way for this new technology to replace the traditional one represented by GTO's. The higher operating switching frequencies and the reduction of the snubber circuit supports the GCT usage [1, 2, and 4]. The ability to operate with a self-powered gate driver in the current source systems was a contribution in the GCT usage [5]. Many researchers work to evaluate losses comparison between GTO and GCT which reveals how much GCT is superior to GTO [6] where a half bridge circuit with a clamp diode and inductive load is used. Also, the development of robust insulated gate bipolar transistors operating at higher voltage levels (HVIGBT) makes the decision not easy which device is the best to be used in the medium voltage high power converters. It was proven that HVIGBT's can operate safely with

978-1-4244-1664-6/08/$25.00 ©2008 IEEE

relatively high switching frequency in snubber-less mode up to 5MW inverter [7, 8]. Many researches compare different semiconductors from losses point of view. GTO and HVIGBT were compared in voltage source inverter mode [9] while HVIGBT and GCT were compared using a clamp circuit and same operating conditions [10].

Other researchers compare HVIGBT, GCT and ETO (emitter turn off thyristor) using pulse-tester circuit [11, 12]. In [13], SGCT and AGCT were compared when utilized in PWM-CSI assuming 50% turn-off and 50% recovery.

In this paper, the losses comparison for medium voltages (2.4 kV, 3.3 kV and 6.6 kV) PWM-CSR is investigated. For each voltage level, conduction losses, on-switching, off-switching and recovery losses for each device are calculated. Moreover, a comparison from size point of view is considered.

I. Arrangement of PWM CSR Devices

For each voltage level there is more than one possibility for selection of the converter's semiconductor half leg. Table I describes the blocking voltage needed for each voltage level [14].

TABLE I
Required Blocking Voltage for PWM-CSR Per Half Leg

Nominal line voltage	Preferred repetitive blocking voltage
2.4 kV	6.5 kV
3.3 kV	9 kV
6.6 kV	18 kV

In the case of current source rectifiers, each device used in these types of converters must have reverse blocking capabilities. This is not a problem in case of SGCT. But in the case of HVIGBT and AGCT, the introduction of series diodes with the switch is mandatory since those switches do not have reverse blocking capabilities. Fig.3 shows different semiconductor combination for PWM-CSR half leg.

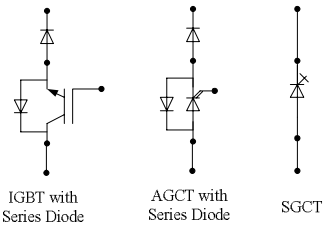

Fig. 3: PWM-CSR half leg utilizing different types of semiconductors

Table II shows the different semiconductor combinations for each voltage level per half-leg of a PWM-CSR in medium voltage systems according to the blocking voltages given in Table I. Those combinations will be compared with each other from the losses point of view. Note that similar devices may be series connected to achieve the required blocking voltage.

The selection of devices from different vendors is as follows in Table III.

TABLE II
Different Semiconductor Combination for Half Leg of Medium Voltage PWM-CSR

Nominal line voltage	HVIGBT	SGCT	AGCT
2.4 kV	1 x 6.5kV HVIGBT + 2 x 4.5kV series diode	1 x 6.5kV SGCT	2 x 4.5kV AGCT + 2 x 4.5kV series diode
3.3 kV	2 x 4.5kV HVIGBT + 2 x 4.5kV series diode	2 x 6.5kV SGCT	2 x 4.5kV AGCT + 2 x 4.5kV series diode
6.6 kV	3 x 6.5kV HVIGBT + 3 x 6kV series diode	3 x 6.5kV SGCT	4 x 4.5kV AGCT + 3 x 6kV series diode

TABLE III
Selected Semiconductors

Device type	Device voltage	Manufacturer	Part number
HVIGBT	4.5kV	DYNEX	DIM600NSM45F000 [19]
Diode	4.5kV	DYNEX	DFM600NXM45F000 [20]
AGCT	4.5kV	ABB	5SHY35L4510 [16]
SGCT	6.5kV	MITSUBISHI	GCU08BA130 [21]
HVIGBT	6.5kV	ABB	5SNA0600G650100 [17]
Diode	6kV	ABB	5SDF10H6004 [18]

II. Semiconductor Losses

The major losses occur in semiconductor devices are classified into two types:

- Conduction losses
- Switching losses

Those losses are interpreted into temperature rise of the semiconductor junction temperature. The losses calculation are essential in the power converters design in order to select the suitable device for each power rating and select the suitable heat sink. Before studying the losses, voltage and current waveforms for each half leg configuration in PWM-CSR using SHE technique are shown in Fig. 4. A PWM-CSR is simulated three times each time utilizing a different semiconductor configuration for its half legs. The system is simulated to operate at 3.3 kV line voltage and supplying a DC link current of 150 A. Single (not series) devices are used in each half leg for the following simulation to simplify the analysis. The purpose of this simulation is to show how the devices are gated and respond to the system voltages and currents. Also, periods of conduction and switching losses can be easily illustrated specially the difference between the off-switching and the recovery losses.

A. Conduction Losses

The conduction power losses during the on-state of a semiconductor device is the product of the current flowing during on-state ($I_{on\text{-}state}$) and the voltage drop at this desired current level ($V_{on\text{-}state}$).

$$P_{conduction} = V_{on-state} \times I_{on-state} \quad (1)$$

The on-state voltage depends on the current flowing through the device. The output characteristic of the device at maximum junction temperature can be used to calculate the conduction losses for different current levels. In order to simplify the analysis, the output characteristic is linearly interpolated [15].

In order to calculate the average conduction power of a switch, this can be done by multiplicating the average on-state current by the on-state voltage at this current level as described by Equation (2).

$$P_{conduction\_average} = V_{on-state-average} \times I_{on-state\_average} \quad (2)$$

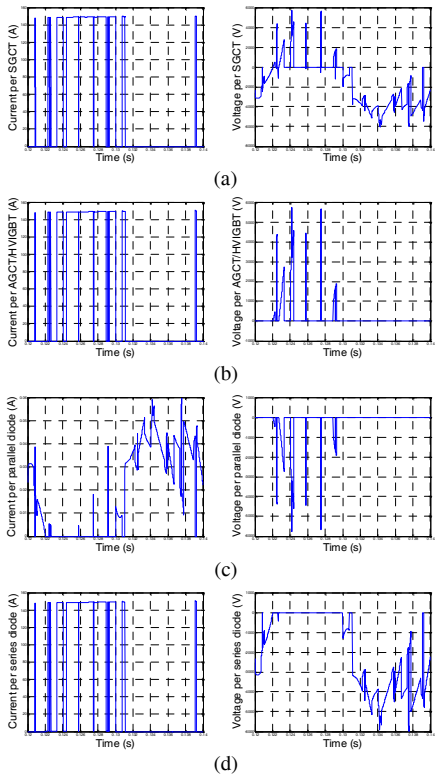

Fig. 4: Voltage and current waveforms for half leg in a PWM-CSR (a) Single SGCT is used as a half leg, (b) Single AGCT/HVIGBT with antiparallel diode and series diode are used as a half leg, (c) Antiparallel accompanying the AGCT/HVIGBT, and (d) Series diode with AGCT/HVIGBT

In the linearized on-state relation, one must substitute with the average current flowing in the switch in $I_{on\text{-}state}$ part. Care must be taken not to exceed the device peak current. For example, a PWM-CSR supplying 150A DC link current at modulation index equals 1, the average current per switch is 50A while the peak current in the switch is 150A assuming ripple free DC link current.

The calculation of the conduction losses is performed by the following steps:

1. The relation between the on-state voltage and the on-state current is determined from the device data sheet [16-21] as shown in Fig. 5.
2. The on-state relation is linearized to simplify the calculations as described in Equation (3) – Equation (8).

$$V_{on-state-6.5kV-SGCT} = 5.5\times10^{-3}\times I_{on-state} + 3.1 \quad (3)$$

$$V_{on-state-4.5kV-HVIGBT} = 2.8\times10^{-3}\times I_{on-state} + 1.65 \quad (4)$$

$$V_{on-state-6.5kV-HVIGBT} = 3.75\times10^{-3}\times I_{on-state} + 3.625 \quad (5)$$

$$V_{on-state-4.5kV-AGCT} = 1\times10^{-3}\times I_{on-state} + 0.7 \quad (6)$$

$$V_{on-state-4.5kV-series\_diode} = 3.5\times10^{-3}\times I_{on-state} + 1.1 \quad (7)$$

$$V_{on-state-6kV-series-diode} = 0.66\times10^{-3}\times I_{on-state} + 1.34 \quad (8)$$

3. The conduction losses are calculated by substitution in Equation (2). For a current range from 100A-600A DC link current, the variation of the conduction losses with the DC link current is shown in Fig. 6.

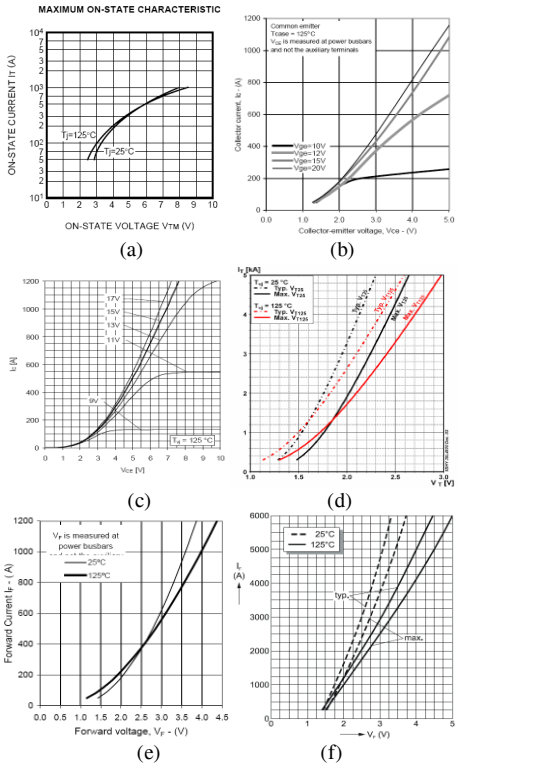

Fig. 5: Relation between on-state voltage and on-state current for (a) 6.5 kV SGCT, (b) 4.5 kV HVIGBT, (c) 6.5 kV HVIGBT, (d) 4.5 kV AGCT, (e) 4.5 kV Fast diode and (f)6 kV Fast diode

B. Switching Losses

No simple expression can be found for the voltage and current during a switching transient. The datasheet parameters concerning the switching losses have to be used in this case. These parameters are referenced to a specific test circuit that simulates a clamped inductive load operated with a specific diode. In actual power circuit the diode used might be different than the diode specified in the datasheet. In this case the calculation of turn-on losses has to be made using the parameters of this particular diode [15].

B.1 On-switching Losses

The calculation of the on-switching losses is performed by the following steps:

1. The relation between the on-switching energy and the turn-on current is determined from the device data sheet [16-21] as illustrated in Fig. 7.

Note that the relation between the on-switching energy and the turn-on current for AGCT is determined from the device data sheet as indicated in Fig. 5 (d). The relation is linearized by interpolation due to the lack of curves in the data sheet. Also, the on-switching losses are neglected for the series fast recovery diodes [1, 14].

2. The on-switching losses relation is linearized to simplify the calculations as described in Equation (9) - Equation (12). The current substituted in Equation (9) - Equation (12) is the peak current at the instant of

the turn on.

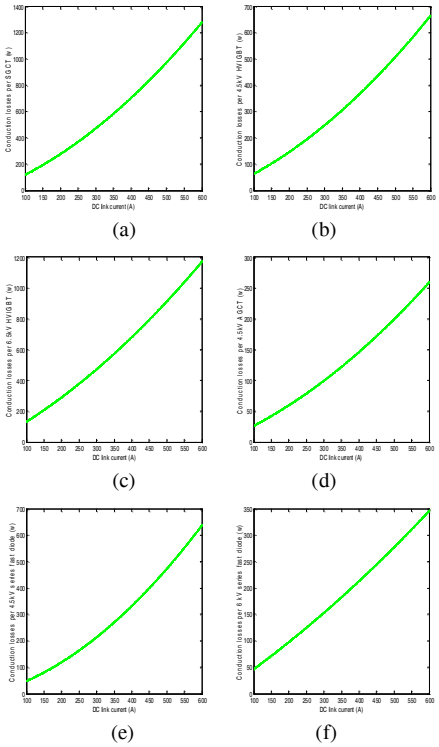

(a) (b) (c) (d) (e) (f)

Fig. 6: Variation of the conduction losses with DC link current
(a) 6.5 kV SGCT, (b) 4.5 kV HVIGBT, (c) 6.5 kV HVIGBT, (d) 4.5 kV AGCT, (e) 4.5 kV Fast diode, and (f) 6 kV Fast diode

$$E_{on-switching-6.5kV-SGCT} = 1\times10^{-3}\times I_{turn-on} + 0.2 \quad (9)$$

$$E_{on-switching-4.5kV-HVIGBT} = 5\times10^{-3}\times I_{turn-on} - 0.25 \quad (10)$$

$$E_{on-switching-6.5kV-HVIGBT} = 7.9\times10^{-3}\times I_{turn-on} + 0.0357 \quad (11)$$

$$E_{on-switching-4.5kV-AGCT} = 0.375\times10^{-3}\times I_{turn-on} \quad (12)$$

3. The on-switching energy can be converted to power losses by multiplying the energy losses with the frequency of switching. As mentioned previously, the system examined utilizes SHE technique to eliminate 5th, 7th and 11th harmonics. Therefore, each switch is pulsed 11 times per cycle (fundamental frequency is 50HZ). The on-switching power loss as a function of the turn-on current is expressed in Equation (13) - Equation (16).

$$P_{on-switching-6.5kV-SGCT} = f_{fundamental}\times N\times(1\times10^{-3}\times I_{turn-on} + 0.2) \quad (13)$$

$$P_{on-switching-4.5kV-HVIGBT} = f_{fundamental}\times N\times(5\times10^{-3}\times I_{turn-on} - 0.25) \quad (14)$$

$$P_{on-switching-6.5kV-HVIGBT} = f_{fundamental}\times N\times(7.9\times10^{-3}\times I_{turn-on} + 0.0357) \quad (15)$$

$$P_{on-switching-4.5kV-AGCT} = f_{fundamental}\times N\times(0.375\times10^{-3}\times I_{turn-on}) \quad (16)$$

Where N is the number of pulses per switch in each cycle according to the SHE technique.

4. The on-switching power losses are calculated by substitution in Equation (13) - Equation (16) for a current range from 100A-600A DC link current. The variation of the conduction losses with the DC link current is shown in Fig. 8

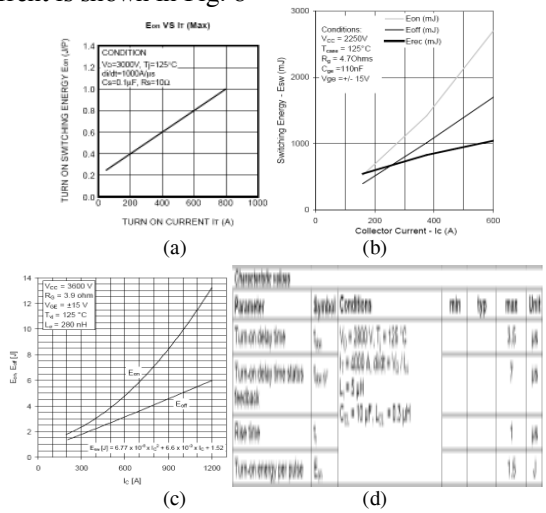

(a) (b) (c) (d)

Fig. 7: Relation between on-switching energy and turn-on current
(a) 6.5 kV SGCT, (b) 4.5 kV HVIGBT, (c) 6.5 kV HVIGBT and (d) 4.5 kV AGCT

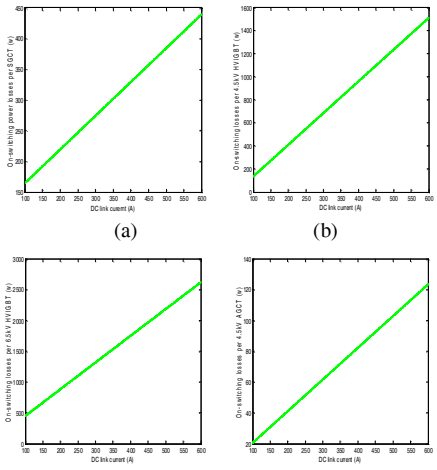

(a) (b) (c) (d)

Fig. 8: Variation of the on switching losses with DC link current
(a) 6.5 kV SGCT, (b) 4.5 kV HVIGBT, (c) 6.5 kV HVIGBT and (d) 4.5 kV AGCT

B.2 Off/Recovery Switching Losses

SGCT has reverse blocking capability. Therefore, it has two possibilities for the off losses. The first is the off-switching losses which occurs if the device is off and forward biased. While, the second is the recovery-switching losses which occurs if the device is off and reverse biased. So, when calculating the off losses, care must be taken whether the device is off-switched or recovered to select the appropriate losses curve to use.

For the HVIGBT, there is only one possibility for the off losses which is the off-switching losses as the device can not withstand reverse voltage. Therefore, when used in application requires reverse voltage capabilities like current source converters, series diodes are used to block the reverse voltage and protect HVIGBT. When the device is off and reverse biased, the series diode will suffer from recovery losses. This is the same case of AGCT. As shown in Fig. 4(a), the SGCT is

subjected to 4 times recovery and 7 times turn-off during one complete cycle. While in the case of HVIGBT, the states at which the current is cut due to the off state of the HVIGBT and it is forward biased are counted in the off-switching losses calculations. As shown in Fig. 4(b), only 7 states are considered for the off-switching calculations. The remainder 4 states (of the total 11 pulses per cycle) are considered in the recovery losses of the fast diode in series with HVIGBT. At these states HVIGBT has very small negative voltage across its terminal which is the on-state voltage of the free-wheeling diode. The case of AGCT is similar to that of HVIGBT.

The calculation of the off/recovery switching losses is performed by the following steps:

1. The relation between the off/recovery switching energy and the turn-on current is determined from the device data sheet [16-21] as shown in Fig. 9.

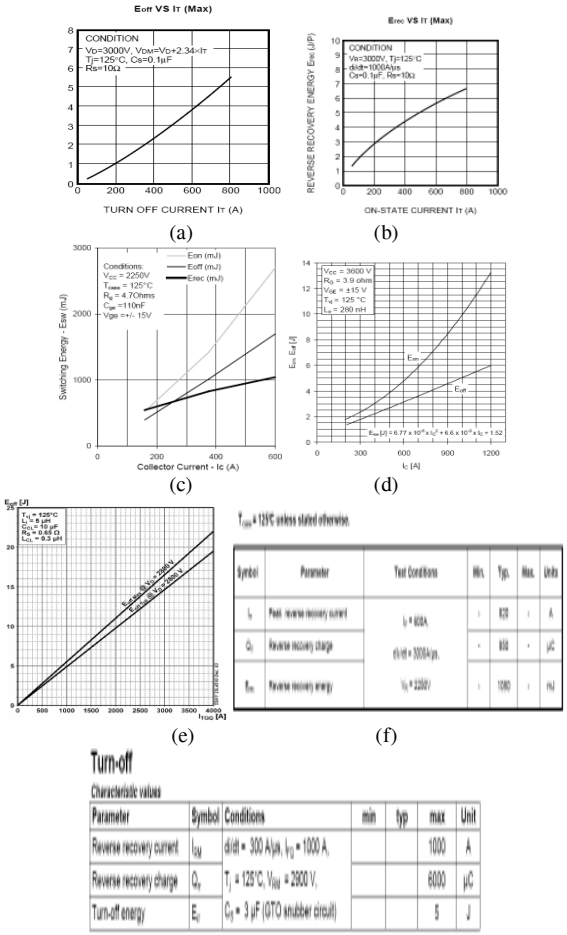

Fig. 9: Relation between off/recovery switching energy and turn-on current
(a) 6.5 kV SGCT, (b) 6.5 kV SGCT, (c) 4.5 kV HVIGBT, (d) 6.5 kV HVIGBT, (e) 4.5 kV AGCT, (f) 4.5 kV Fast diode and (g) 6 kV Fast diode

Note that the relation between the recovery-switching energy and the turn-on current for series diodes is determined from the device data sheet as shown in Fig. 9 (f) and (g). The relation is linearized by interpolation due to the lack of curves in the data sheet.

2. The off-switching losses and the recovery-switching losses relations are linearized to simplify the calculations as described in Equation (17)-Equation (23).

$$E_{off-switching-6.5kV-SGCT} = 7\times10^{-3}\times I_{turn-on} - 0.4 \quad (17)$$

$$E_{rec-switching-6.5kV-SGCT} = 7\times10^{-3}\times I_{turn-on} + 1.4 \quad (18)$$

$$E_{off-switching-4.5kV-HVIGBT} = 3.12\times10^{-3}\times I_{turn-on} - 0.125 \quad (19)$$

$$E_{off-switching-6.5kV-HVIGBT} = 5\times10^{-3}\times I_{turn-on} \quad (20)$$

$$E_{off-switching-4.5kV-AGCT} = 5.75\times10^{-3}\times I_{turn-on} - 0.12 \quad (21)$$

$$E_{rec-switching-4.5kV-series-diode} = 1.8\times10^{-3}\times I_{turn-on} \quad (22)$$

$$E_{rec-switching-6kV-series-diode} = 5\times10^{-3}\times I_{turn-on} \quad (23)$$

The current substituted in Equation in Equation (17)-Equation (23) is the peak current at the instant of the turn on.

3. The off-switching and recovery-switching energy can be converted to power losses by multiplying the energy losses with the frequency of switching. The off-switching and recovery-switching power losses as a function of the turn-on current are expressed in Equation (24)-Equation (30).

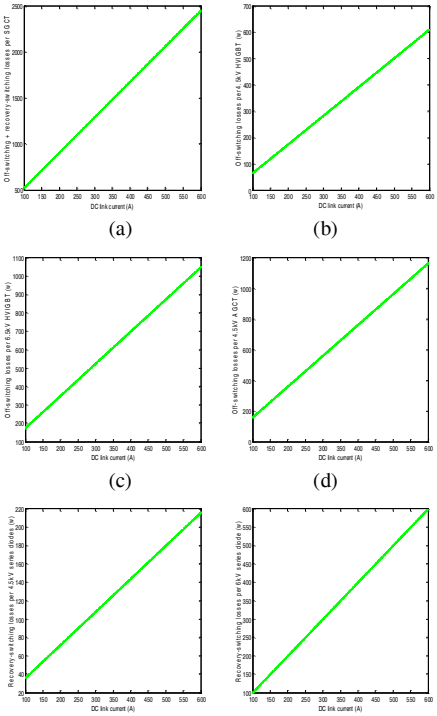

Fig. 10: Variation of the off/recovery witching losses with DC link current
(a) 6.5 kV SGCT, (b) 4.5 kV HVIGBT, (c) 6.5 kV HVIGBT, (d) 4.5 kV AGCT, (e) 4.5 kV Fast diode, and (f) 6 kV Fast diode

$$P_{off-switching-6.5kV-SGCT} = f_{fundamental}\times N_{off}\times(7\times10^{-3}\times I_{turn-on} - 0.4) \quad (24)$$

$$P_{rec-switching-6.5kV-SGCT} = f_{fundamental}\times N_{rec}\times(7\times10^{-3}\times I_{turn-on} + 1.4) \quad (25)$$

$$P_{off-switching-4.5kV-HVIGBT} = f_{fundamental}\times N_{off}\times(3.12\times10^{-3}\times I_{turn-on} - 0.125) \quad (26)$$

$$P_{off-switching-6.5kV-HVIGBT} = f_{fundamental}\times N_{off}\times(5\times10^{-3}\times I_{turn-on}) \quad (27)$$

$$P_{off-switching-4.5kV-AGCT} = f_{fundamental}\times N_{off}\times(5.75\times10^{-3}\times I_{turn-on} - 0.12) \quad (28)$$

$$P_{rec-switching-4.5kV-series-diode} = f_{fundamental}\times N_{rec}\times(1.8\times10^{-3}\times I_{turn-on}) \quad (29)$$

$$P_{rec-switching-6kV-series-diode} = f_{fundamental} \times N_{rec} \times (5\times10^{-3} \times I_{turn-on}) \quad (30)$$

Where,

N_{off} is the number of pulses, in each cycle according to the SHE technique, during which the switch is off while it is forward biased.

N_{rec} is the number of pulses, in each cycle according to the SHE technique, during which the switch is off while it is reverse biased.

4. The off-switching and recovery-switching power losses are calculated by substitution in Equation (24)-Equation (30). For a current range from 100A-600A DC link current, the variation of the off/recovery losses with the DC link current is shown in Fig. 10.

III. Results and Discussion

According to the previous losses calculations, different semiconductors are compared from losses point of view to find out what is the suitable configuration for each medium voltage level. Also, the size of the semiconductors is taken into consideration.

A. 2.4 kV System

Fig. 11 shows that minimum losses are acquired using the SGCT combination (1x 6.5kV SGCT) for current ranges 200A up to 600A. The current range from 100A-200A the AGCT combination is the minimum but the configuration is complicated as it uses 2 x 4.5 kV AGCT and 2 x 4.5 kV series diode compared to the single IGCT configuration. In the range 200A-600A, the SGCT configuration is the best from the losses and number of devices points of view. To clarify the size point of view, referring to data sheets [16, 17, 20 and 21], the size of the rectifier half leg is illustrated in Table. IV

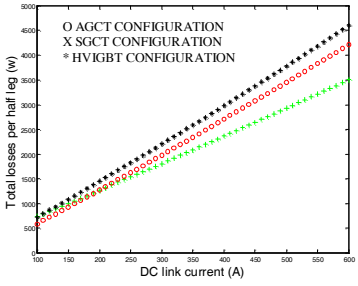

Fig. 11: Variation of the total losses with DC link current for 2.4 kV system

Although losses in case of AGCT seem to be equal to that of SGCT, rectifiers built with SGCT are 33% the size of their equivalent built with AGCT. In case of SGCT and AGCT, the size includes the firing circuit which is built on board. For HVIGBT, it is assumed that the firing circuit is half the module size. Although the HVIGBT size seems to be larger than that of SGCT, the overall topology with HVIGBT will be smaller in size than SGCT since HVIGBT module has three devices in the same module which will be used in the other legs of the rectifier.

TABLE IV
Size Calculation for 2.4 kV System

Configuration	SGCT	AGCT	HVIGBT
Switching devices required	1	2	1
Switching devices per module	1	1	3
Module size (mm^2)	$52x10^3$	$75.947x10^3$	$26.6\ x10^3$
Series diodes required	0	2	2
diodes per module	-	2	2
Module size (mm^2)	-	$16.12\ x10^3$	$16.12\ x10^3$
Total size (mm^2)	$52\ x10^3$	$168.04\ x10^3$	$29.42\ x10^3$

B. 3.3 kV System

Fig. 12 shows that minimum losses are acquired using the AGCT combination (2 x 4.5 kV AGCT and 2 x 4.5 kV series diode). The AGCT configuration and the HVIGBT configuration utilize the same type of series diodes. But the conduction losses and the on-switching losses of AGCT are lower than that of HVIGBT as shown previously in Fig.6 and Fig.8 respectively. Ratio of losses AGCT:HVIGBT:SGCT is 1:1.8:1.8 at 600A while HVIGBT and AGCT losses seem to be equal at low current rating (up to 150A). From the size point of view, referring to data sheets [16, 19, 20 and 21], the size of the rectifier half leg is calculated as shown in Table. V

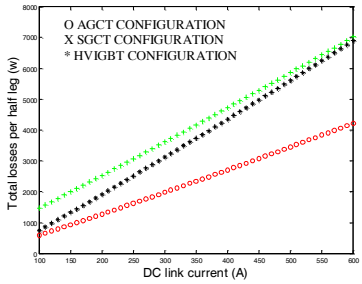

Fig. 12: Variation of the total losses with DC link current for 3.3 kV system

It is clear that HVIGBT configuration is the smallest in size. HVIGBT makes the rectifier 23% smaller than its size of a similar one built using AGCT. In the whole current range, AGCT is the best from losses point of view, HVIGBT is the best from size point of view and SGCT is the best from number of devices point of view.

B. 6.6 kV System

Fig. 13 shows that minimum losses are acquired using the AGCT combination (4 x 4.5 kV AGCT and 3 x 6 kV series diode). But, one must notice that the difference in power losses between this configuration and the one utilizes SGCT (3 x 6.6 kV SGCT) is not very large compared to the large number of series devices used in the AGCT configuration. Ratio of losses AGCT:HVIGBT:SGCT is 1:1.86:1.3 at 600A. From the size point of view, referring to data sheets [16, 17, 18 and 21], the size of the rectifier half leg is calculated as shown in Table. VI.

TABLE V
SIZE CALCULATION FOR 3.3 KV SYSTEM

Configuration	SGCT	AGCT	HVIGBT
Switching devices required	2	2	2
Switching devices per module	1	1	2
Module size (mm^2)	52 $x10^3$	75.947 $x10^3$	16.12 $x10^3$
Series diodes required	0	2	2
diodes per module	-	2	2
Module size (mm^2)	-	16.12 $x10^3$	16.12 $x10^3$
Total size (mm^2)	104 $x10^3$	168.04 $x10^3$	40.3 $x10^3$

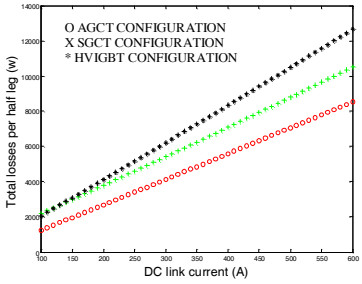

Fig. 13: Variation of the total losses with DC link current for 6.6 kV system

TABLE VI
SIZE CALCULATION FOR 6.6 KV SYSTEM

Configuration	SGCT	AGCT	HVIGBT
Switching devices required	3	4	3
Switching devices per module	1	1	3
Module size (mm^2)	52e3 $x10^3$	75.947 $x10^3$	26.6 $x10^3$
Series diodes required	0	3	3
diodes per module	-	1	1
Module size (mm^2)	-	7.014 $x10^3$	7.014 $x10^3$
Total size (mm^2)	156 $x10^3$	324.8 $x10^3$	60.92 $x10^3$

IV. CONCLUSION

For each voltage level and current range, there is one best selection of semiconductors from a losses point of view. This selection may not meet other considerations, like size and number of devices. The selection varies with the working voltage level and current range.

The results of the calculations and comparisons presented in this paper are in Table. IX.

TABLE IX
SEMICONDUCTOR SELECTION FROM DIFFERENT POINTS OF VIEW

Voltage level	Minimum losses	Minimum size	Minimum Number of devices
2.4 kV	AGCT (100A-200A) SGCT (200A-600A)	HVIGBT	SGCT
3.3 kV	AGCT	HVIGBT	SGCT
6.6 kV	AGCT	HVIGBT	SGCT

REFERENCES

[1] Wu, B.: 'High Power Converter Systems' (IEEE Press and John Wiley, March 2006)

[2] Zargari, N.R., Rizzo, S.C., Xiao, Y., Iwamoto, H., Satoh, K., and Donlon, J.F.: 'A New Current Source Converter Using a Symmetric Gate-Commutated Thyristor (SGCT)', IEEE Trans. Industry Applications, June 2001, vol. 37, pp. 896 – 903

[3] Rizzo, S.C., Wu, B., and Sotudeh, R.: 'Symmetric GTO and Snubber Component Characterization in PWM Current Source Inverters', IEEE Trans. Power Electronics, July 1998, vol. 13, pp. 617–525

[4] Stillman, H.M.: 'IGCTs - Megawatt Power Switches for Medium Voltage Applications', ABB Review, 1997, No. 3, pp. 12-17

[5] Hu, W., Wu, B., Zargari, N.R., and Cheng, Z.: 'A Novel Self-Powered Supply for GCT Gate Drivers'. Twenty Second Annual IEEE Applied Power Electronics Conference APEC 2007, Anaheim, CA, USA, February 2007, pp. 1275 - 1279.

[6] Donton, J.F., Motto, E.R., Yamamoto, M., and Takahiko L.: 'A New Gate Commutated Turn-off Thyristor and Companion Diode for High Power Applications'. Thirty Third IAS Annual Meeting, October 1998, vol.2, pp. 873 - 880

[7] Lai, J., Leslie, L., Ferrell, J., and Nergaard, T.: 'Characterization of HV-IGBT for High-Power Inverter Applications'. Fourtieth IAS Annual Meeting, Hong Kong, China, October 2005, vol. 1, pp. 377 – 382

[8] Dieckerhoff, S., Bernet, S., and Krug, D.: 'Power Loss-Oriented Evaluation of High Voltage IGBTs and Multilevel Converters in Transformerless Traction Applications', IEEE Trans. Power Electronics, November 2005, vol. 20, pp. 1328 – 1336

[9] Satoh, K., Yamamoto, M., Morishita, K., Yamaguchi, Y., and Iwamoto, H.: 'High Power Symmetrical GCT for Current Source Inverter'. International Conference on Power Electronics and Drive Systems PEDS'99, Hong Kong, China, July 1999, pp. 877 - 882

[10] Zargari, N.R., Rizzo, S.C., Xiao, Y., Iwamoto, H., Satoh, K., and Donlon, J.F.: 'Comparison of High Hower IGBT's and Hard-Driven GTO's for High Power Inverters', IEEE Trans. Industry Applications, March 1999, vol. 35, pp. 487-493

[11] Satoh, K., Nakagawa, T., Yamamoto, M., Morishita K., and Kawakami, A.: '6kV/4kA Gate Commutated Turn-off Thyristor with Operation DC Voltage of 3.6kV'. International Symposium on Power Semiconductor Devices and ICs ISPSD'98, Kyoto, Japan, June 1998, pp. 205-208

[12] Huang, A.Q., Motto, K., and Li, Y.: 'Development and Comparison of High-Power Semiconductor Switches'. International Power Electronics and Motion Control Conference IPEMC 2000, Beijing, China, August 2000, vol.1, pp. 70 - 78

[13] Motto, K., Li, Y., and Huang, A.Q.: 'Comparison of the State-of-the-art High Power IGBTs, GCTs and ETOs'.Applied Power Electronics Conference and Exposition APEC 2000, New Orleans, LA, USA, February 2000, vol.2, pp. 1129 - 1136

[14] http://search.abb.com/library/Download.aspx?DocumentID=5SYA2051%2D00&LanguageCode=en&DocumentPartID=&Action=Launch&IncludeExternalPublicLimited=True, accessed March 2008

[15] http://www.infineon.com/dgdl/anip031e.pdf?folderId=db3a304412b407950112b4092c730139&fileId=db3a304412b407950112b40a4d3e04ff, accessed March 2008

[16] http://library.abb.com/GLOBAL/SCOT/scot256.nsf/VerityDisplay/26934990889C13DCC1256FF10022622A/$File/5SHY%2035L4510_5SYA1232-02June%2007.pdf, accessed March 2008

[17] http://search.abb.com/library/Download.aspx?DocumentID=5SYA1558%2D02&LanguageCode=en&DocumentPartID=&Action=Launch&IncludeExternalPublicLimited=True, accessed March 2008

[18] http://library.abb.com/GLOBAL/SCOT/scot256.nsf/VerityDisplay/9196CF9A51D4490CC12572340048251F/$File/5SDF%2010H6004_5SYA1109-02Oct%2006.pdf, accessed March 2008

[19] http://www.dynexsemi.com/assets/IGBT_Modules/Datasheets/DNX_DIM600NSM45-F000.pdf, accessed March 2008

[20] http://www.dynexsemi.com/assets/FRD_Modules/Datasheets/DNX_DFM600NXM45-F000.pdf, accessed March 2008

[21] http://www.mitsubishichips.com/China/content/product/power/thyristors/gct/gct/gcu08ba-130_e.pdf, accessed March 2008